

Mercury-Sensitized Photochemical Vapor Deposition of Amorphous Silicon

A reaction engineering model has been developed to describe the mercury-sensitized photochemical vapor deposition of hydrogenated amorphous silicon (a-Si:H) semiconductor thin films. Model equations governing the gas-phase generation, transport, and surface reactions of SiH_3 and H film precursor radicals are solved to predict film growth rate and bonded hydrogen content. Behavior of the model has been studied as a function of deposition conditions (pressure, temperature, feed composition, and flow rates) and has been verified by comparison with experimental results.

D. E. Albright
N. Saxena
C. M. Fortmann
R. E. Rocheleau
T. W. F. Russell

Department of Chemical Engineering
and Institute of Energy Conversion
University of Delaware
Newark, DE 19716

Introduction

Thin-film semiconductors have the potential for significant advantages over single-crystal semiconductors through lower cost and greater adaptability to mass production. One of the most promising materials is hydrogenated amorphous silicon (a-Si:H) which has applications in solar cells, thin-film transistors, photosensitive diodes, and photoreceptors (LeComber, 1987; Wronski, 1988; Carlson, 1989). Amorphous silicon thin films suitable for applications in electronic devices are commonly deposited by plasma-assisted chemical vapor deposition (Catalano et al., 1983). Alternate techniques including chemical vapor deposition (Bogaert, 1986), reactive sputtering (Ross and Messier, 1981), direct photochemical vapor deposition (Yamada, 1985), and mercury-sensitized photochemical vapor deposition (Rocheleau et al., 1987) have also been reported. Mercury-sensitized photo-CVD has produced a-Si:H alloys and devices which are comparable to those deposited by plasma-CVD. Mercury-sensitized photo-CVD shares many of the same growth phenomena as plasma-CVD, but offers the advantages of well defined gas-phase chemistry and kinetics. Thus, mercury-sensitized photo-CVD serves as an excellent model system for developing an understanding of the film formation process.

The fabrication of thin-film electronic devices requires control of film growth rate and optoelectronic properties. The optoelectronic properties of a-Si:H films depend to a large extent on hydrogen content (Adler, 1985; LeComber, 1987). To control growth rate and hydrogen content it is necessary to quantitatively understand the effects of operating conditions (pressure,

temperature, feed composition, and flow rates) on the film deposition process. To this end, a reaction engineering model of a mercury-sensitized photo-CVD reactor, which quantifies the kinetic and transport processes to predict film growth rate and hydrogen content, has been developed. The model is presently being used to control the growth rate and hydrogen content of a-Si:H solar cell layers in an on-going investigation sponsored by the Solar Energy Research Institute (SERI). The model has been extremely valuable in directing changes in process conditions and minimizing the necessary amount of experimental effort.

Reactor

A schematic of the mercury-sensitized photo-CVD reactor designed and constructed at the University of Delaware is shown in Figure 1. The reactor is divided into two chambers by a UV-transparent Teflon curtain. Reactant gases and mercury vapor flow through the lower chamber over heated substrates. Ultraviolet light (253.7 nm) from a low-pressure mercury vapor lamp initiates mercury-sensitized decomposition of the reactants to form radicals. These radicals diffuse to the substrates, the curtain, and the reactor walls depositing as film. Since deposition on the curtain attenuates incoming light, the curtain is rolled at regular intervals (typically two minutes) by a computer-controlled system. The upper chamber eliminates deposition on the quartz window by using argon to flush away reactants which diffuse around the curtain.

Films are deposited from silane diluted in hydrogen or helium. Flow rates through the reaction chamber are controlled by calibrated mass flow controllers and range from 2 to 100 std. cm^3/min . Deposition pressures range from 67 to 1,330 Pa and are controlled with an accuracy of 25 Pa using a capacitance

Correspondence concerning this paper should be addressed to T. W. F. Russell.
R. E. Rocheleau is presently with the Hawaii Natural Energy Institute, University of Hawaii, Honolulu, HI 96822.

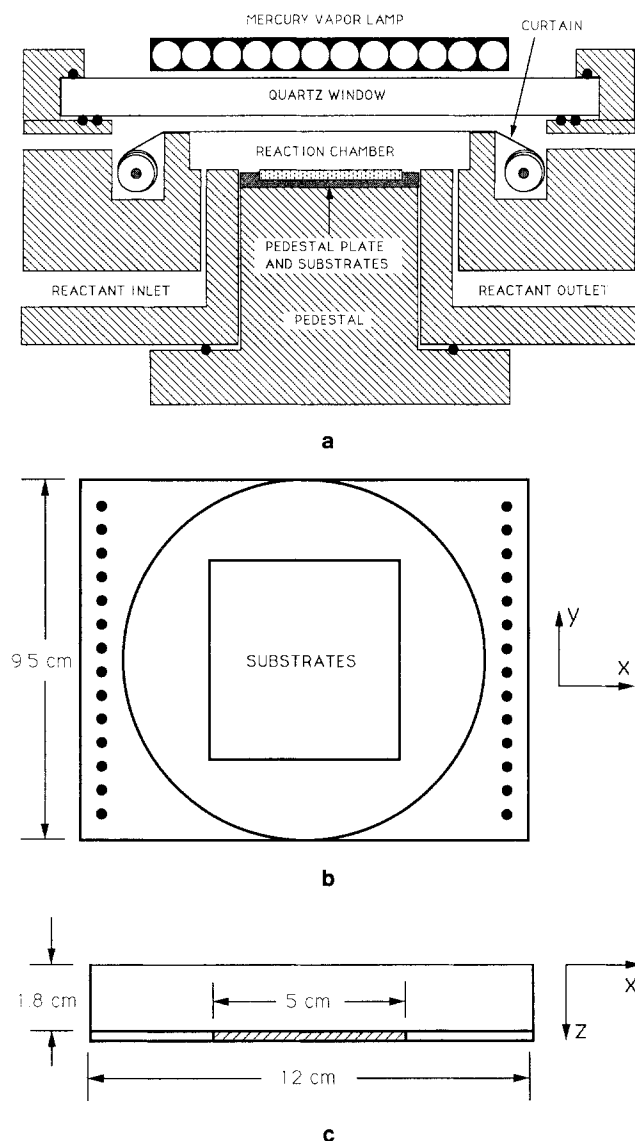


Figure 1. Mercury-sensitized photo-CVD reactor.

- 1a. Photo-CVD reactor.
1b. Top view of reaction chamber.
1c. Side view of reaction chamber.

manometer and controller system. Electronic quality films are typically deposited between 205 and 230°C, although a range of substrate temperatures from 40 to 230°C have been studied as part of the experimental effort to understand and quantify the surface reactions. Substrate temperatures are calibrated and maintained with an estimated accuracy of 10°C.

Film Analysis

Average film growth rates at the substrate are determined by measuring film thickness using a surface profiler (estimated accuracy of ± 15 nm) and dividing by the total deposition time. Since curtain growth causes variations in the light intensity entering the reaction chamber, curtain transmissions are measured and average growth rates normalized to a fixed light intensity of 6.3 mW/cm², which is the 253.7 nm light intensity measured at the top of the reaction chamber without a curtain. Normalization is possible since the film growth rate was

experimentally determined to be directly proportional to light intensity under our operating conditions. Film hydrogen content is measured by secondary ion mass spectroscopy (SIMS) and by Fourier transform infrared (FTIR) spectroscopy (estimated accuracy of $\pm 20\%$).

Model Development

Gas-phase chemistry

The simplified gas-phase chemistry describing the mercury-sensitized photo-CVD process is shown in Table 1. Ultraviolet photons (253.7 nm) are absorbed by mercury vapor exciting the ground-level Hg(¹S₀) to an excited triplet-state Hg(³P₁), referred to as Hg*. The Hg* atom is 469.4 kJ/mol above the ground state (Calvert and Pitts, 1966). This excess energy can be transferred to the silane and hydrogen via collision, leading to the generation of SiH₃ and H radicals and the quenching of Hg* back to the ground state (Niki and Mains, 1964; Yarwood et al., 1964; Kamaratos and Lampe, 1970). H radicals formed by the reaction of Hg* with silane and hydrogen can further react with silane to form SiH₃ radicals and molecular hydrogen (Austin and Lampe, 1977). No reaction occurs with helium (Callear, 1987) which is used only to control reactant concentrations. Hg* can also quench to the ground state by the spontaneous emission of a photon.

The rate constants of mercury-sensitized reactions are usually expressed in terms of an effective quenching cross-section, σ^2 , to be used in conjunction with the kinetic theory collision rate equation so that the second-order rate constant for quenching (k_2 or k_3 in Table 1) is given by:

$$k_Q = \sigma_Q^2 \sqrt{8\pi RT_g} \left(\frac{1}{M_{\text{Hg}}} + \frac{1}{M_Q} \right) \quad (1)$$

where the subscript, *Q*, refers to the quenching gas (silane or hydrogen) and *T_g* is the gas-phase temperature. A quenching cross-section for silane of 0.45 nm² was recommended by Yarwood et al. (1964). This is in agreement with the recently measured value of 0.54 ± 0.05 nm² (Perrin and Allain, 1988) which has been adopted for this work. The reported quenching cross-sections of hydrogen are 0.098 nm² (Yarwood et al., 1964), 0.108 ± 0.005 nm² (Gleditsch and Michael, 1975), and 0.102 ± 0.005 nm² (Perrin and Allain, 1988). A value of 0.102 nm² has been adopted.

While studies of the reaction of H radicals with silane using microwave discharge and direct photolysis to generate hydrogen radicals have been reported (Mihelcic et al., 1977), reaction rate constants determined using mercury sensitization are most appropriate for this work since the other techniques can impart

Table 1. Simplified Gas-Phase Chemistry

$\text{Hg} + (253.7 \text{ nm photon}) \rightarrow \text{Hg}^*$
$\text{Hg}^* \xrightarrow{k_1} \text{Hg} + (253.7 \text{ nm photon})$
$\text{Hg}^* + \text{SiH}_4 \xrightarrow{k_2} \text{SiH}_3 + \text{H} + \text{Hg}$
$\text{Hg}^* + \text{H}_2 \xrightarrow{k_3} \text{H} + \text{H} + \text{Hg}$
$\text{H} + \text{SiH}_4 \xrightarrow{k_4} \text{SiH}_3 + \text{H}_2$

excess energy to the hydrogen radicals generated. A rate constant for the reaction of H radicals with silane, k_4 , of 2.6 E11 mol/cm³/s at 305 K with an activation energy of 10.4 kJ/mol has been adopted (Austin and Lampe, 1977). This is in good agreement with 2.65 E11 mol/cm³/s determined at room temperature (Worsdorfer et al., 1983).

When present in large concentrations, it is possible for SiH₃ radicals to recombine in the gas phase initiating complex secondary reactions which form disilane (Si₂H₆) and higher polymers (Becerra and Walsh, 1987). Due to the low radical concentrations used in this work, these reactions are neglected in developing the model.

Gas-phase mass balance

The flow through the reaction chamber is fully developed and laminar with negligible free convection under all operating conditions. Since the reactor is operated at low conversions (less than 15%), and the gas-phase diffusivities are large (100 to 1,000 cm²/s), concentration gradients in the feed gases are negligible. Therefore, only the transport of the radical species needs to be considered. The steady-state gas-phase mass balance describing the generation and transport of SiH₃ and H is shown in Eq. 2.

$$-D_j \nabla^2 C_j + \nabla(V C_j) = R_j \quad (2)$$

The convection term can be neglected for radicals since the characteristic time for diffusion to the curtain or the substrate (h^2/D) is much less than that necessary for significant convection to occur in the x direction (L/V_x).

Light intensity is uniform in the x-y plane, but varies in the z direction due to absorption by mercury. Since the concentrations of stable species are constant throughout the reaction chamber, radical generation rates vary only in the z direction. Due to the aspect ratios of the reaction chamber, the only significant wall reactions occur at the substrate and the curtain. Combined, these facts imply that radical concentration gradients are only important in the z direction.

If these ordering arguments are correct, there should be no variations in composition or growth rate with position on the substrates. Experimentally determined film thicknesses had a standard deviation of less than 5% over the entire substrate area. FTIR measurements showed no detectable variations in the hydrogen content with position. Since negligible growth rate and composition variations were observed, the experimental results are consistent with the ordering arguments presented.

With the ordering argument simplifications described above, Eq. 2 can be rewritten as

$$-D_j \frac{d^2 C_j}{dz^2} = R_j \quad (3)$$

where R_j is the net gas-phase generation rate of radical species j . For SiH₃ and H, R_j is given by the constitutive relationships:

$$R_{\text{SiH}_3} = k_2[\text{SiH}_4][\text{Hg}^*] + k_4[\text{SiH}_4][\text{H}] \quad (4)$$

$$R_{\text{H}} = 2k_3[\text{Hg}^*][\text{H}_2] + k_2[\text{Hg}^*][\text{SiH}_4] - k_4[\text{H}][\text{SiH}_4] \quad (5)$$

To solve Eqs. 4 and 5, the steady-state concentration profile of Hg* must be determined. Hg* is generated by the absorption of a 253.7 nm photon supplied either by the lamp or by spontaneous emission from another Hg* atom within the reaction chamber. The Hg* is deactivated either by collision with a reactant molecule or by spontaneous emission of a photon. Since the Hg* is deactivated (characteristic time of 1 E-6 s) before any significant diffusion can take place (characteristic time of 1 E-4 s), the transport is negligible and the steady-state profile of Hg* can be determined simply from the positionally dependent generation and loss rates. The equations used to quantify the concentration of Hg* in the reaction chamber as a function of the z position are described in detail by Perrin and Broekhuizen (1987a).

After the Hg* concentration profile is calculated, the concentration of the radical species is determined by solving Eqs. 6 and 7:

$$-D_{\text{SiH}_3} \frac{d^2[\text{SiH}_3]}{dz^2} = k_2[\text{SiH}_4][\text{Hg}^*] + k_4[\text{SiH}_4][\text{H}] \quad (6)$$

$$-D_{\text{H}} \frac{d^2[\text{H}]}{dz^2} = 2k_3[\text{Hg}^*][\text{H}_2] + k_2[\text{Hg}^*][\text{SiH}_4] - k_4[\text{H}][\text{SiH}_4] \quad (7)$$

The boundary conditions for these equations equate the flux of each species at the surface to its rate of reaction at the surface.

$$D_j dC_j/dz|_{z=0} = r(\text{rxn}, j) \quad (8)$$

$$-D_j dC_j/dz|_{z=h} = r(\text{rxn}, j) \quad (9)$$

where $r(\text{rxn}, j)$ = reaction rate of component j at the surface evaluated at the curtain for ($z = 0$) or at the substrate for ($z = h$).

Gas-phase boundary conditions

At the curtain or substrate, the accumulation of SiH₃ and H is given by:

$$\frac{1}{A} M_j \frac{dm_j}{dt} = r(i, j) - r(r, j) - r(\text{rxn}, j) \quad (10)$$

where

A = area of film, cm²

$r(i, j)$ = incident flux rate of component j , mol/cm²/s

$r(r, j)$ = reflection rate of component j , mol/cm²/s

Since at steady state there is no accumulation of gas phase species on the surface, the left hand side of Equation 10 is zero and the rate of reaction is equal to the net flux to the surface. The reaction rate can be expressed as a fraction of the incident flux estimated by kinetic theory:

$$r(\text{rxn}, j) = r(i, j) - r(r, j) = \beta_j r(i, j) = \beta_j (v_j)(C_j/4) \quad (11)$$

where β_j is the probability that radical j (SiH₃ or H) will react upon a single collision with the surface ($0 \leq \beta_j \leq 1$) and v_j =

$(8RT_g/\pi M_j)^{1/2}$. The reaction rates of SiH_3 and H at the curtain and the substrate in Eqs. 8 and 9 are then given by:

$$r(\text{rxn}, \text{SiH}_3) = \beta_{\text{SiH}_3}(v_{\text{SiH}_3}[\text{SiH}_3])/4 \quad (12)$$

$$r(\text{rxn}, \text{H}) = \beta_{\text{H}}(v_{\text{H}}[\text{H}])/4 \quad (13)$$

Equations 6 to 9, 13 and 14 completely describe the photo-CVD system and are solved to obtain the net reaction rates of SiH_3 and H at the substrate and the curtain. In these equations, the gas-phase reactions and appropriate rate constants are known from the literature. The gas-phase diffusion coefficients are estimated using Chapman-Enskog theory and the Lennard-Jones parameters for each species (Reid et al., 1987; Matsui et al., 1987). For depositions between 50 and 350°C, β_{SiH_3} varies between 0.1 and 0.2, while β_{H} varies between 0.6 and 0.8 (Perrin and Broekhuizen, 1987b). The gas temperature is assumed to be the same as the substrate temperature at 25°C and 85% of the substrate temperature when the substrate is at 265°C. Sensitivity of the model to gas temperature is examined later in the text to determine the effect of this assumption. A numerical software package is used to solve Eqs. 6 and 7 with boundary conditions given by substituting Eqs. 13 and 14 into Eqs. 8 and 9.

Surface mass balance

To model the film formation process, a specific surface chemistry must be proposed. Since little is known about the film formation process, it is possible to postulate chemical equations having any degree of complexity. Since the surface concentrations cannot be measured and the mechanisms cannot be verified, a simplified set of surface reactions directly linked to measurable quantities such as growth rate and composition has been chosen, Table 2. Si_{film} and H_{film} are the silicon and hydrogen incorporated in the film and Z_{H} is the net number of hydrogen (between 0 and 3) incorporated into the film with each SiH_3 radical.

The model predicts that the flux of SiH_3 and H at the surface is linearly dependent on the 253.7 nm light intensity. By varying the 253.7 nm light intensity, it has been experimentally determined that the incorporation rate of silicon is linearly dependent on the flux of SiH_3 radicals at the surface. It has also been experimentally determined that the silicon removal rate is linearly dependent on the flux of H atoms at the surface. Since the net reaction rates of SiH_3 and H are predicted by Eqs. 13 and 14, it is convenient to express the contribution of each surface reaction as a fraction of the flux of the particular radical species. S_1 is defined as the fraction of the SiH_3 surface flux which reacts via (SR1). Thus,

$$S_1 = \frac{\text{reaction rate of SiH}_3 \text{ via SR1}}{r(\text{rxn}, \text{SiH}_3)} \quad (14)$$

Table 2. Simplified Surface Chemistry

<i>Film formation:</i>	
$\text{SiH}_3 \rightarrow (\text{Si}_{\text{film}} + Z_{\text{H}} \text{H}_{\text{film}}) + (3-Z_{\text{H}})/2 \text{H}_2$	(SR1)
$\text{H} \rightarrow \text{H}_{\text{film}}$	(SR2)
<i>Film removal by etching:</i>	
$\text{H} + (\text{Si}_{\text{film}} + 3 \text{H}_{\text{film}}) \rightarrow \text{SiH}_4$	(SR3)

S_2 and S_3 are the fractions of the H surface flux which react via (SR2) and (SR3).

$$S_2 = \frac{\text{reaction rate of H via SR2}}{r(\text{rxn}, \text{H})} \quad (15)$$

$$S_3 = \frac{\text{reaction rate of H via SR3}}{r(\text{rxn}, \text{H})} \quad (16)$$

The surface mass balances are given by:

$$\frac{1}{A} \frac{d\text{Si}_{\text{film}}}{dt} = S_1 \beta_{\text{SiH}_3}(V_{\text{SiH}_3}[\text{SiH}_3])/4 - S_3 \beta_{\text{H}}(V_{\text{H}}[\text{H}])/4 \quad (17)$$

$$\frac{1}{A} \frac{d\text{H}_{\text{film}}}{dt} = (Z_{\text{H}} S_1) \beta_{\text{SiH}_3}(V_{\text{SiH}_3}[\text{SiH}_3])/4 + (S_2) \beta_{\text{H}}(V_{\text{H}}[\text{H}])/4 \quad (18)$$

The growth rate is then calculated from:

$$\text{Growth rate} \left(\frac{\text{nm}}{\text{s}} \right) = \frac{1}{\rho_{\text{film}}} \left(\frac{1}{A} M_{\text{Si}} \frac{d\text{Si}_{\text{film}}}{dt} \right) 10^7 \quad (19)$$

where the a-Si:H density, ρ_{film} , ranges from about 2.0 to 2.3 g/cm³ as the film hydrogen content is increased from 0 to 20% (Mahan, 1990). The hydrogen content of the film is given by:

$$\text{atomic \% hydrogen in film} = \left(\frac{\frac{d\text{H}_{\text{film}}}{dt}}{\frac{d\text{Si}_{\text{film}}}{dt} + \frac{d\text{H}_{\text{film}}}{dt}} \right) * 100 \quad (20)$$

A quantitative model similar to that presented has been developed by Perrin and Broekhuizen (1987b). The present model extends this work in two ways. First, the present model accounts for the hydrogen incorporation from SiH_3 and H radicals. Thus, it can predict film hydrogen content, whereas Perrin and Broekhuizen dealt only with silicon accumulation. Secondly, this model includes the etching reaction of H radicals, whereas this was not considered in the previous work.

Model Behavior

General trends with pressure, dilution, and temperature

Figure 2 shows the model-predicted SiH_3 and H radical fluxes at the substrate as a function of deposition pressure for 10% silane in helium and 10% silane in hydrogen at 230°C. The flux of SiH_3 at the substrate decreases, while flux of H radicals increases with decreasing pressure for both dilutions. The flux of H to the surface is greater than the flux of SiH_3 only for depositions using hydrogen dilution at low pressures. The gas-phase model is fairly insensitive to operating temperature. At a given pressure and feed composition, the predicted radical fluxes at the surface vary less than 30% between 40 and 250°C.

Sensitivity to rate constants and surface reaction probability

The sensitivity of the model predictions to gas-phase rate constants is generally found to be small over the range reported

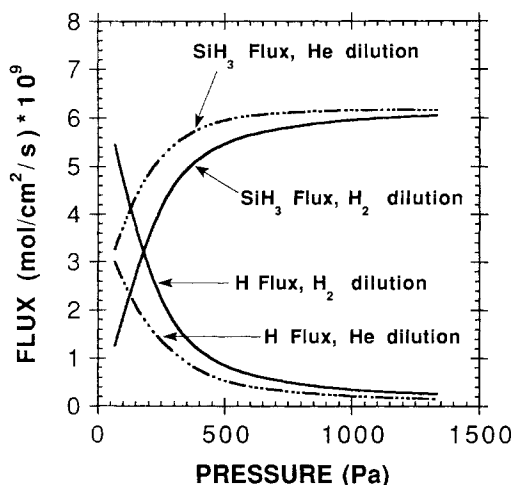


Figure 2. Predicted radical fluxes at the substrate as a function of pressure for deposition from 10% silane in helium and 10% silane in hydrogen at 230°C.

in the literature. The most significant effect on model predictions is seen by varying the rate constant for the reaction of hydrogen with silane, k_4 . The size of this effect depends on the operating pressure and dilution. For depositions from pure silane or silane diluted in helium, changes in k_4 have almost no effect over the pressure range 67 to 1,330 Pa. With 10% silane diluted in hydrogen, the maximum effect of k_4 is seen at 67 Pa where the predicted H flux decreases by 20% as k_4 is increased by a factor of two. Changes in the model predicted fluxes are negligible when the Hg^* quenching cross sections used to determine the reaction rate constants for silane and hydrogen, k_2 and k_3 , are varied over the range reported in the literature. The model predicted fluxes of H and SiH_3 to the surface are also found to be insensitive to β_{SiH_3} and β_H over the range 0.1 to 1, since the predicted radical concentrations just above the surface change inversely with the chosen β so that the righthand side of Eqs. 13 and 14 remain constant.

Sensitivity to measured mercury concentration

The reactor was designed to control the mercury concentration by passing the individual feed gases (SiH_4 , H_2 , and He) over heated mercury reservoirs. The gas-phase mercury concentration in our reaction chamber has been measured to be approximately 5 E13 molecules/cm³ over a wide range of operating pressures and flow rates. Since 5 E13 molecules/cm³ is approximately the room-temperature-saturated value, excess mercury apparently condenses in the room temperature inlet yielding a feed gas to the reactor saturated with mercury at room temperature. Although varying the mercury concentration over the estimated experimental error (2.5 E13 to 7.5 E13 molecules/cm³) causes rather large variations in the predicted Hg^* concentration profile, the predicted reaction rates of SiH_3 and H at the substrate vary less than 20% for the operating conditions used in this work due to the smoothing effects of the large diffusivities.

Experimental Quantification of Surface Reactions

Since the surface reaction parameters S_1 through S_3 are ratios of reaction rates which may contain complex activation energy

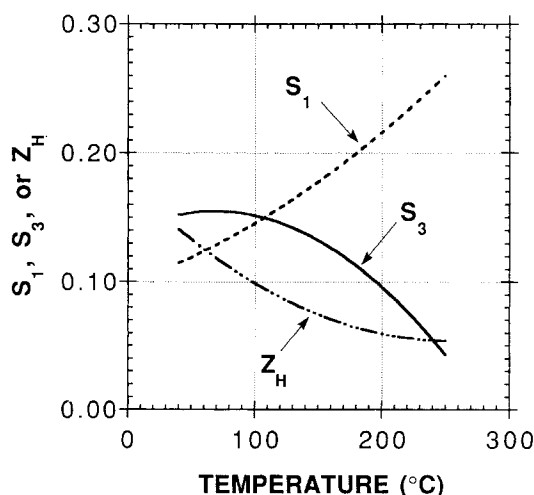


Figure 3. S_1 , S_3 , and Z_H as a function of temperature.

terms, they are expected to be functions of surface temperature. Since Z_H is dependent on hydrogen incorporation and elimination reactions for film growth from SiH_3 , it is also expected to be temperature-dependent. At a given substrate temperature, a single set of parameters should be able to predict the film growth rate and hydrogen content for all pressures and feed gas compositions. S_1 was determined by comparing the predicted SiH_3 flux with the experimentally determined growth rate at 667 Pa, where the model predicts a negligible contribution from hydrogen radicals. S_3 was determined by comparing the etching rate of freshly deposited a-Si:H films with the model predicted flux of hydrogen radicals under etching conditions (70 Pa, pure H_2). Z_H was determined from the experimentally measured hydrogen content for depositions at 667 Pa, where the model predicts a negligible H flux. Figure 3 shows the determined values of S_1 , S_3 , and Z_H as a function of substrate temperature. S_2 was determined by comparing the model predicted and experimentally determined film hydrogen content under conditions, where the model predicts the H surface flux to be approximately equivalent to the SiH_3 flux. S_2 is very small and was determined only in the temperature range used to produce

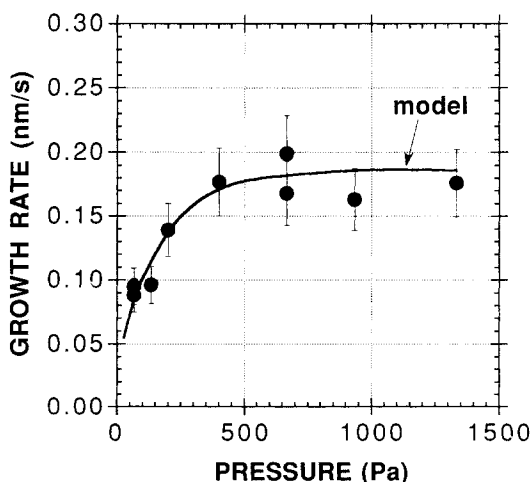


Figure 4. Film growth rate as a function of pressure for deposition from 10% silane in helium at 230°C.

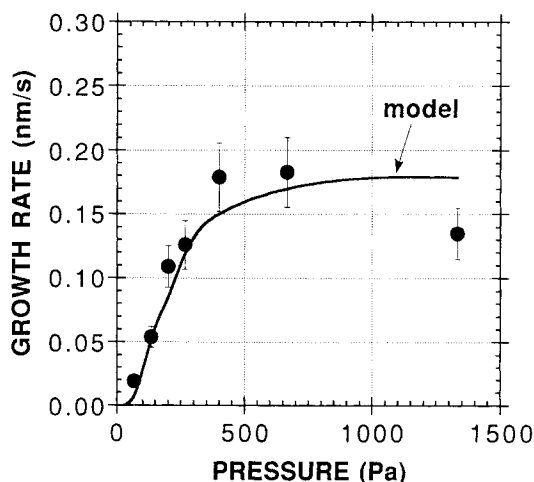


Figure 5. Film growth rate as a function of pressure for deposition from 10% silane in hydrogen at 230°C.

electronic quality films ($S_2 = 0.0015$ at 230°C and $S_2 = 0.003$ at 205°C).

Comparison of Model Predictions with Experimental Data

Depositions were made at 205 and 230°C over a range of pressures and dilutions to compare the model behavior with experimental results (Figures 4 through 9). In all cases, the model predicted growth rates and hydrogen contents were consistent with the experimentally determined values. The comparison of model-predicted and experimentally-measured growth rates as a function of pressure for 10% silane in helium and 10% silane in hydrogen dilution at 230°C is shown in Figures 4 and 5, respectively. Experimental film growth rate as a function of deposition pressure for 20% silane in helium at 205°C is compared with model predictions in Figure 6.

Comparison of model-predicted hydrogen contents with experimental data are shown in Figures 7 through 9. For the hydrogen diluted depositions shown in Figure 8, operation below 267 Pa

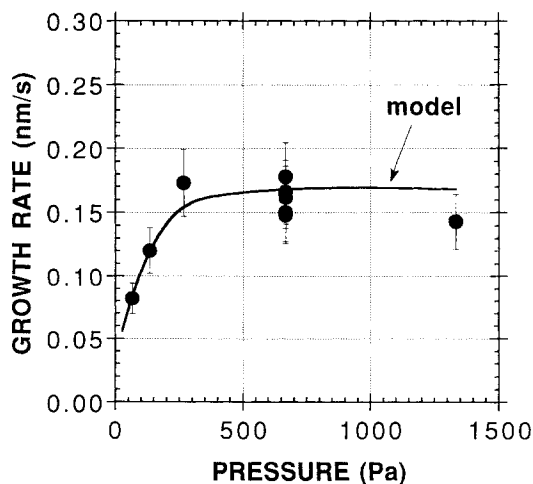


Figure 6. Film growth rate as a function of pressure for deposition from 20% silane in helium at 205°C.

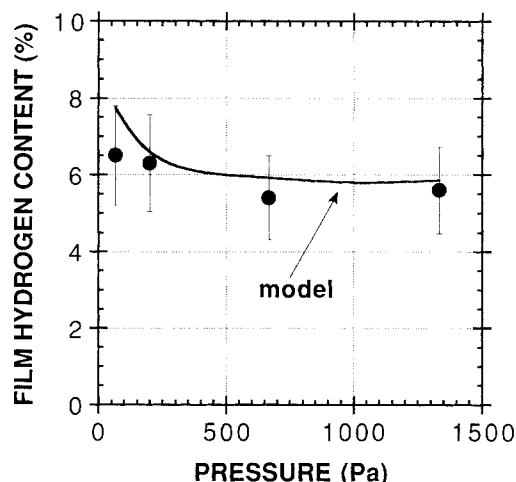


Figure 7. Film hydrogen content as a function of pressure for deposition from 10% silane in helium at 230°C.

produced microcrystalline films and is therefore not modeled. The experimentally-observed shift from amorphous silicon to microcrystalline silicon with decreasing pressure (and thus increasing H radical flux) has been previously discussed (Saxena et al., 1989).

Conclusion

A reaction engineering model has been developed to describe the mercury-sensitized photochemical vapor deposition of a-Si:H. This model quantifies the reactions of SiH_3 and H at the surface during film formation to predict film growth rate and hydrogen content as a function of pressure, temperature, and feed gas composition. Model behavior has shown good agreement with experimental data. The ability to control film growth rate and hydrogen incorporation through the operating parameters (pressure, temperature, and gas phase composition) allows the thickness and composition of device structures to be tailored with a minimal amount of experimental effort. We have found

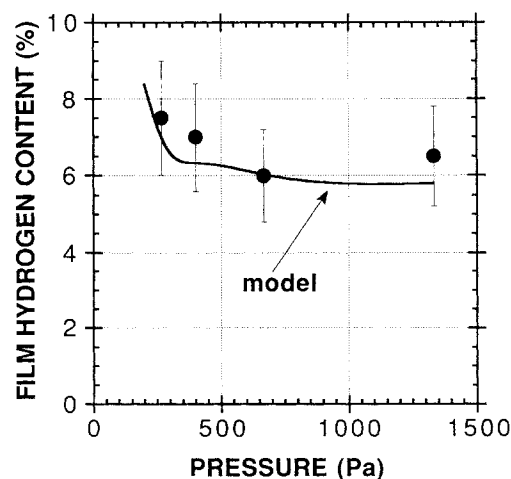


Figure 8. Film hydrogen content as a function of pressure for deposition from 10% silane in hydrogen at 230°C.

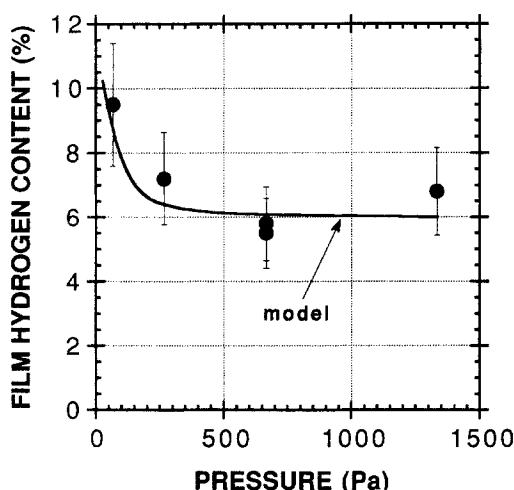


Figure 9. Film hydrogen content as a function of pressure for deposition from 20% silane in helium at 205°C.

the model extremely useful as a tool in research efforts to develop stable, high-efficiency a-Si:H solar cells.

Acknowledgment

This work was partially supported by the Solar Energy Research Institute under subcontract #XL-8-18092-1 and by Graduate Fellowship (D. E. Albright from the Amoco Foundation). We also acknowledge the Center for Composite Materials at the University of Delaware for the use of their FDIR Spectrophotometer.

Notation

- A = area of film, cm^2
- C_j = gas-phase concentration of species j , mol/cm^3
- D_j = gas-phase diffusivity of species j , cm^2/s
- h = height of the reaction chamber, cm
- H_{film} = bonded hydrogen in the film, mol
- Hg^* = excited triplet state of mercury, $\text{Hg}(^3P_1)$
- k_j = rate constant for gas phase reaction j
- L = flow direction length of the reaction chamber, cm
- m_j = accumulated mass of species j , g
- M_j = molecular weight of species j , g/mol
- R = ideal gas constant
- R_j = reaction rate of species j in the gas phase, $\text{mol}/\text{cm}^3/\text{s}$
- $r(i, j)$ = incidence rate of species j at the surface, $\text{mol}/\text{cm}^2/\text{s}$
- $r(r, j)$ = reflection or emission rate of species j from the surface, $\text{mol}/\text{cm}^2/\text{s}$
- $r(\text{rxn}, j)$ = reaction rate of species j at the surface, $\text{mol}/\text{cm}^2/\text{s}$
- S_1, S_2, S_3 = ratios of reaction rates defined by Eqs. 15, 16 and 17, respectively
- Si_{film} = bonded silicon in the film, mol
- T_g = temperature of the gas phase, K
- V = convective velocity, cm/s
- v_j = gas-phase kinetic theory velocity of species j , cm/s
- x, y, z = coordinate directions defined in Figure 1
- Z_H = number of hydrogen which incorporate into the film with each SiH_3
- β_j = probability that species j will react upon a single collision with the surface
- ρ_{film} = density of a-Si:H film, g/cm^3
- σ^2 = $\text{Hg}(^3P_1)$ quenching cross section, nm^2

Literature Cited

- Adler, D., "Chemistry and Physics of Covalent Amorphous Semiconductors," *Physical Properties of Amorphous Materials*, D. Adler, B. B. Schwartz, and M. C. Steele, eds., Plenum Press, p. 5 (1985).
- Austin, E. R., and F. W. Lampe, "Rate Constants for the Reactions of Hydrogen Atoms with Some Silanes and Germanes," *J. Phys. Chem.*, **81**, 1134 (1977).
- Becerra, R., and R. Walsh, "Mechanism of Formation of Tri- and Tetrasilane in the Reaction of Atomic Hydrogen with Monosilane and the Thermochemistry of the Si_2H_4 Isomers," *J. Phys. Chem.*, **91**, 5765 (1987).
- Bogaert, R. J., "Chemical Vapor Deposition of Amorphous Silicon Films from Disilane," PhD Dissertation, Univ. of Delaware (1986).
- Callear, A. B., "Excited Mercury Complexes," *Chem. Rev.*, **87**, 335 (1987).
- Calvert, J. C., and J. N. Pitts, *Photochemistry*, Wiley, New York (1966).
- Carlson, D. E., "Amorphous-Silicon Solar Cells," *IEEE Trans. Electr. Dev.*, **36**, 2775 (1989).
- Catalano, A., P. A. Longeway, H. A. Weakliem, "Chemistry of Silane Discharges," *RCA Engr.*, **28**, 50 (1983).
- Gleditsch, S. D., and J. V. Michael, "Further Mercury (3P_1) Quenching Cross Sections," *J. Phys. Chem.*, **79**, 409 (1975).
- Kamaratos, E., and F. W. Lampe, "A Mass Spectrometric Study of the Mercury-Photosensitized Reactions of Silane and Methylsilane with Nitric Oxide," *J. Phys. Chem.*, **74**, 2267 (1970).
- LeComber, P. G., "Applications and Defects in Amorphous Silicon," *J. Non-Cryst. Solids*, **90**, 219 (1987).
- Matsui, Y., A. Yuuki, N. Morita, and K. Tachibana, "On the Reaction Kinetics in a Mercury Photosensitized CVD of a-Si:H Films," *Jap. J. Appl. Phys.*, **26**, 1575 (1987).
- Mahan, A. H., private communication, Solar Energy Research Institute.
- Mihelcic, D., V. Schubert, R. N. Schindler, and P. Potzinger, "Rate Constants for the Reaction of Hydrogen and Deuterium Atoms with Silane," *J. Phys. Chem.*, **81**, 1543 (1977).
- Niki, H., and G. J. Mains, "The 3P_1 Mercury-Photosensitized Decomposition of Monosilane," *J. Phys. Chem.*, **68**, 304 (1964).
- Perrin, J., and B. Allain, "Quenching of Excited Mercury Atoms (6^3P_1 and 6^3P_0) in Collisions with SiH_4 , SiD_4 , Si_2H_6 and GeH_4 ," *J. Chem. Phys.*, **123**, 295 (1988).
- Perrin, J., and T. Broekhuizen, "Radiative Transfer in Mercury-Sensitized Photochemical Vapor Deposition," *J. Quant. Spectrosc. Radiat. Transfer*, **38**, 369 (1987a).
- , "Surface Reaction and Recombination of the SiH_3 Radical on the Hydrogenated Amorphous Silicon," *Appl. Phys. Lett.*, **50**, 433 (1987b).
- Reid, R. C., J. M. Prausnitz, and B. E. Poling, *The Properties of Gases & Liquids*, 4th ed., McGraw-Hill, New York (1987).
- Rocheleau, R. E., S. S. Hegedus, W. A. Buchanan, and S. C. Jackson, "Novel Photochemical Vapor Deposition Reactor for Amorphous Silicon Solar Cell Deposition," *Appl. Phys. Lett.*, **51**, 133 (1987).
- Ross, R. C., and R. Messier, "Microstructure and Properties of rf-Sputtered Amorphous Hydrogenated Silicon Films," *J. Appl. Phys.*, **52**, 5329 (1981).
- Saxena, N., D. E. Albright, C. M. Fortmann, T. W. F. Russell, P. Fauchet, and I. H. Campbell, "Temperature Dependence of H Radical Etching in the Deposition of Microcrystalline Silicon Alloy Thin Films by Hg-Sensitized Photo-CVD," *J. Non-Cryst. Solids*, **114**, 801 (1989).
- Worsdorfer, K., B. Reimann, and P. Potzinger, "The Reaction of Hydrogen Atoms with Silyl Radicals; the Decomposition Pathways of Chemically Activated Silanes," *Z. Naturforsch.*, **38a**, 896 (1983).
- Wronski, C. R., "Amorphous Silicon and Its Applications," *Solid State Technol.*, **31**, 113 (1988).
- Yamada, A., M. Konagai, and K. Takahashi, "Excimer-Laser-Induced Chemical Vapor Deposition of Hydrogenated Amorphous Silicon," *Jap. J. Appl. Phys.*, **24**, 1586 (1985).
- Yarwood, A. J., O. P. Strausz, and H. E. Gunning, "Quenching of the 2537-Å Resonance Radiation of Mercury," *J. Chem. Phys.*, **41**, 1705 (1964).

Manuscript received Mar. 16, 1990, and revision received Aug. 9, 1990.